

established. The interface properties may be improved by different annealing conditions after gate oxide growth [6, 7]. However, a high-temperature anneal would contribute to dopant diffusion.

© IEE 2001

28 August 2001

Electronics Letters Online No: 20011039
DOI: 10.1049/el:20011039

U.N. Straube, A.M. Waite and A.G.R. Evans (*ECS Department, University of Southampton, Southampton, SO17 1BJ, United Kingdom*)
E-mail: uns97r@ecs.soton.ac.uk

A. Nejjim and P.L.F. Hemment (*School of Electronic Engineering, Information Technology and Mathematics, University of Surrey, Guildford, GU2 5XH, United Kingdom*)

References

- 1 STRAUBE, U.N., EVANS, A.G.R., BRAITHWAITE, G., KAYA, S., WATLING, J., and ASENOV, A.: 'On the mobility extraction for HEMOSFETs', *Solid-State Electron.*, 2001, **45**, (3), pp. 527–529
- 2 SIDEK, R.M., STRAUBE, U.N., WAITE, A.M., EVANS, A.G.R., PARRY, C., PHILLIPS, P., WHALL, T.E., and PARKER, E.H.C.: 'SiGe CMOS fabrication using SiGe MBE and anodic/LTO gate oxide', *Semicond. Sci. Technol.*, 2000, **15**, pp. 135–138
- 3 CHRISTIANO, F., NEJJIM, A., SUPRUN-BELEVICH, Y., CLAVERIE, A., and HEMMENT, P.L.F.: 'Formation of extended defects and strain relaxation in ion beam synthesised SiGe alloys', *Nucl. Instrum. Methods Phys. Res. B*, 1999, **147**, pp. 35–42
- 4 JIANG, H., and ELLIMAN, R.: 'Electrical properties of GeSi surface and buried-channel p-MOSFETs fabricated by Ge implantation', *IEEE Trans. Electron Devices*, 1996, **43**, (1), pp. 97–103
- 5 LEGOUES, F.K., ROSENBERG, R., and MEYERSON, B.S.: 'Kinetics and mechanism of oxidation of SiGe: dry versus wet oxidation', *Appl. Phys. Lett.*, 1989, **54**, (7), pp. 644–646
- 6 TCHIKATILOV, D., YANG, Y.F., and YANG, E.S.: 'Improvement of SiGe oxide grown by electron cyclotron resonance using H₂O vapor annealing', *Appl. Phys. Lett.*, 1996, **69**, (17), pp. 2578–2580
- 7 AHN, C.-G., KANG, H.-S., KWON, Y.-K., and KANG, B.: 'Effects of segregated Ge on electrical properties of SiO₂/SiGe interface: Part 1', *Jpn. J. Appl. Phys.*, 1998, **37**, (3B), pp. 1316–1319

Effect of deep traps on sheet charge in AlGaIn/GaN high electron mobility transistors

P.B. Klein, S.C. Binari, K. Ikossi, A.E. Wickenden, D.D. Koleske and R.L. Henry

The same traps that produce current collapse in AlGaIn/GaN high electron mobility transistors are also shown to limit the sheet charge that is attainable in these devices by the trapping of channel carriers at equilibrium (no applied bias). In the present case, this reduction in sheet charge was found comparable to that induced by current collapse.

Introduction: Nitride-based electronic devices are currently of great interest for high power, high frequency and high temperature applications. While excellent device characteristics have been reported for high electron mobility transistors (HEMTs), such performance is not always reproducible owing to the effects of deep trapping centres in the device structures. Traps can produce transient instabilities [1], persistent photoconductivity [2], current collapse/drain lag [3], gate lag [4] and other effects leading to the degradation of device performance. In this Letter, we discuss the effect of deep traps on the sheet charge, n_s , that is achievable in the two-dimensional electron gas (2DEG) of the HEMT device. The concentration of deep centres is varied by changing the pressure during growth (metal organic vapour phase epitaxy (MOVPE)) of the high-resistivity (HR) GaN buffer layer [5, 6].

The sheet charge in HEMT devices that are exposed to a high drain-source voltage can be substantially reduced through the mechanism of current collapse, where hot 2DEG carriers are injected into neighbouring regions of the device structure that contain a large concentration of traps. These carriers can become trapped, and will remain trapped after the high voltage is removed if the traps are deep. This reduction in the sheet charge leads to a

concomitant reduction in the drain current. In nitride-based field effect transistors (FETs), it has been shown [7–9] that two distinct traps (labelled trap 1 and trap 2) are responsible for this effect, and that they reside in the HR-GaN buffer layer. Current collapse can be reversed by light illumination, as the trapped carriers are released by photoionisation and the drain current is restored. Spectroscopic investigation of this effect has been employed to measure the unique photoionisation spectrum associated with each of the traps responsible for current collapse in nitride-based FETs [6–8]. Furthermore, it has been shown that a quantitative measurement of the light-induced increase in the drain current, obtained as a function of the amount of light incident on the device, allows the determination of the areal densities and photoionisation cross-sections of the responsible traps [6, 9]. Consequently, the trap concentrations can be followed as a function of variations in the materials growth and device fabrication parameters [6].

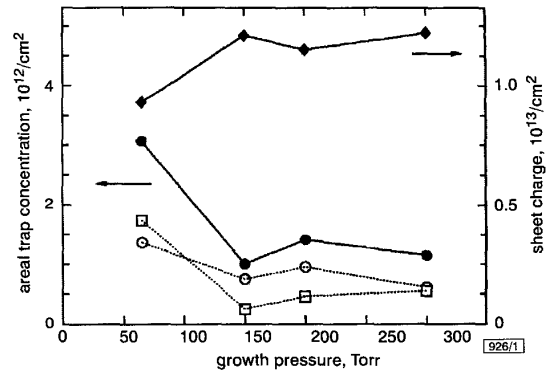


Fig. 1 Variation with MOVPE growth pressure of sheet charge and areal concentration of filled traps [6] responsible for current collapse in AlGaIn/GaN HEMT devices

●— total traps
○--- trap 1
□--- trap 2
◆— sheet charge

Results: A 20 nm AlN nucleation layer was grown on a-plane sapphire substrates, followed by a 3 μm HR-GaN buffer layer. A 25 nm layer of Al_{0.3}Ga_{0.7}N was then grown to form the 2DEG. Four wafers were grown under identical conditions, except for a systematic variation of the HR-GaN growth pressure (65, 150, 200 and 300 Torr) to vary the defect incorporation in the layer. The areal trap concentrations were determined [7] as noted above.

Fig. 1 shows the dependence upon growth pressure of the concentration of each of the two traps causing current collapse, the total trap concentration (their sum) and the sheet charge (measured by Hall effect under conditions where no collapse occurs). From our previous studies, there is evidence [7] that trap 2 is associated with the presence of carbon-related defects, and that trap 1 may be related to grain boundaries or dislocations. Fig. 1 shows that, as a function of growth pressure, the sheet charge and the total trap concentration exhibit an inverse correlation. This behaviour suggests that the measured sheet charge has been reduced by the presence of traps in the HR-GaN. Since the measured trap concentration is that of the traps producing current collapse, it appears that the same species of trap is also responsible for a reduced sheet charge at equilibrium. This is shown more clearly in Fig. 2 which plots sheet charge (n_s) (filled circles) against the total areal concentration of traps responsible for the collapse (n_T). The observed linear relationship supports this view. The extrapolation to the vertical axis, indicated by $n_{s,0}$ in Fig. 2, represents the sheet charge that would be attainable if there were no traps at all in the material.

Discussion: If deep electron traps are present in the HR-GaN during the formation of the 2DEG, it is expected that carriers would be trapped at these centres during growth/cool-down, thus reducing the number of carriers available to the conducting channel. These traps, in the charged region of the HR-GaN adjacent to the 2DEG (defined as region 1, thickness d_{E0}), would be filled at equilibrium. The same species of electron trap outside of this region

(i.e. region 2, below region 1 and deeper into the HR-GaN layer) remains empty at equilibrium, and becomes filled (effective thickness d_{NEQ}) during current collapse by nonequilibrium hot carriers resulting from a high applied drain bias. At equilibrium, the sheet charge is reduced by the areal density of charge trapped in region 1, $n_s = n_{s,0} - N_T d_{EQ}$, where N_T is the volume trap density. During current collapse, region 1 traps remain filled, and the traps in region 2 become filled to an areal density $n_T = N_T d_{NEQ}$, where n_T corresponds to the trap density measured in [6]. The dependence of n_s on n_T is then $n_s = n_{s,0} - (d_{EQ}/d_{NEQ})n_T$. This linear relationship is shown as the solid line in Fig. 2, which is fitted to the data to give $n_{s,0} = 1.36 \times 10^{13}/\text{cm}^2$ and $(d_{EQ}/d_{NEQ}) = 1.38$.

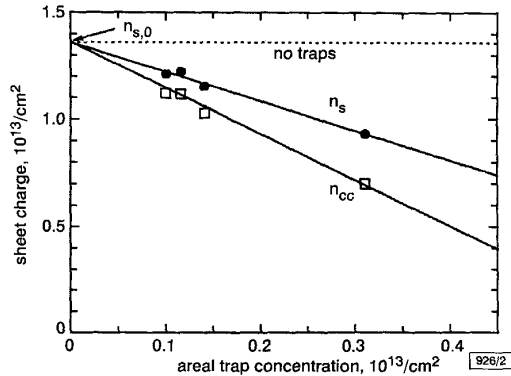


Fig. 2 Dependence of equilibrium sheet charge (n_s) on areal concentration of nonequilibrium filled traps in HR-GaN layer, responsible for current collapse

Similar dependence of sheet charge remaining after current collapse is labelled n_{cc}

The sheet charge after current collapse, n_{cc} , is further reduced by the areal density of trapped charge in region 2: $n_{cc} = n_s - n_T = n_s - N_T d_{NEQ} = n_{s,0} - (1 + d_{EQ}/d_{NEQ})n_T$. This is plotted as the dashed line in Fig. 2, using the values for $n_{s,0}$ and (d_{EQ}/d_{NEQ}) determined above. The experimental points are plotted as the open squares in Fig. 2. Fig. 2 demonstrates that the same species of deep trap in the HR-GaN limits device performance by two independent mechanisms: deep traps filled at equilibrium reduce the attainable 2DEG sheet charge, while those traps that remain empty at equilibrium may be filled during current collapse to further reduce the sheet charge. As d_{EQ}/d_{NEQ} was found to be near unity, we can conclude that in the present study the effective thickness of the two charged regions and their corresponding areal charge densities were comparable.

Acknowledgments: The authors would like to thank J. Albrecht and P.P. Ruden for several helpful discussions. This work was supported in part by the Office of Naval Research.

© IEE 2001
Electronics Letters Online No: 20011040
DOI: 10.1049/el:20011040

24 September 2001

P.B. Klein, S.C. Binari, K. Ikossi and R.L. Henry (Naval Research Laboratory, 4555 Overlook Avenue SW, Washington DC 20375-5347, USA)

E-mail: klein@bloch.nrl.navy.mil

A.E. Wickenden (Army Research Laboratory, Adelphi, MD 20783-1197, USA)

D.D. Koleske (Sandia National Laboratories, Albuquerque, NM 87185, USA)

References

- THEIS, T.N., and WRIGHT, S.L.: 'Origin of "residual" persistent photoconductivity in selectively doped GaAs/Al_xGa_{1-x}As heterojunctions', *Appl. Phys. Lett.*, 1986, **48**, (20), pp. 1374-1376
- HIRSCH, M.T., WOLK, J.A., WALUKIEWICZ, W., and HALLER, E.E.: 'Persistent photoconductivity in n-type GaN', *Appl. Phys. Lett.*, 1977, **71**, (8), pp. 1098-1100
- BINARI, S.C., KRUPPA, W., DIETRICH, H.B., KELNER, G., WICKENDEN, A.E., and FREITAS, J.A., Jr.: 'Fabrication and characterization of GaN FETs', *Solid-State Electron.*, 1997, **41**, (10), pp. 1549-1554

- BINARI, S.C., IKOSSI, K., ROUSSOS, J.A., KRUPPA, W., PARK, D., DIETRICH, H.B., KOLESKE, D.D., WICKENDEN, A.E., and HENRY, R.L.: 'Trapping effects and microwave power performance in AlGaIn/GaN HEMTs', *IEEE Trans. Electron. Dev.*, 2001, **48**, pp. 465-471
- WICKENDEN, A.E., KOLESKE, D.D., HENRY, R.L., GORMAN, R.J., TWIGG, M.E., FATEMI, M., FREITAS, J.A., Jr., and MOORE, W.J.: 'The influence of OMVPE growth pressure on the morphology, compensation, and doping of GaN and related alloys', *J. Electron. Mater.*, 2000, **29**, (1), pp. 21-26
- KLEIN, P.B., BINARI, S.C., IKOSSI, K., WICKENDEN, A.E., KOLESKE, D.D., and HENRY, R.L.: 'Current collapse and the role of carbon in AlGaIn/GaN high electron mobility transistors grown by metalorganic vapor-phase epitaxy', *Appl. Phys. Lett.* (in press)
- KLEIN, P.B., FREITAS, J.A., Jr., BINARI, S.C., and WICKENDEN, A.E.: 'Observation of deep traps responsible for current collapse in GaN metal semiconductor field effect transistors', *Appl. Phys. Lett.*, 1999, **75**, (25), pp. 4016-4018
- KLEIN, P.B., BINARI, S.C., IKOSSI, K., WICKENDEN, A.E., KOLESKE, D.D., and HENRY, R.L.: 'Investigation of traps producing current collapse in AlGaIn/GaN high electron mobility transistors', *Electron. Lett.*, 2001, **37**, (10), pp. 661-662
- KLEIN, P.B., BINARI, S.C., FREITAS, J.A., Jr., and WICKENDEN, A.E.: 'Photoionization spectroscopy of traps in GaN metal semiconductor field effect transistors', *J. Appl. Phys.*, 2000, **88**, (5), pp. 2843-2852

Decision-directed passive phase conjugation: equalisation performance in shallow water

J.A. Flynn, J.A. Ritcey, W.L.J. Fox, D.R. Jackson and D. Rouseff

A decision-directed extension to passive phase conjugation array demodulation is described. Initialisation by a training preamble is followed by block least-squares channel estimation via conjugate gradient and memoryless decisions, which are used by estimation in the next block. Excellent shallow-water performance is shown at ranges up to 4.6 km under windy conditions and shipping noise. The algorithm demonstrates low error rate and robust channel tracking.

Introduction: We describe a novel decision-directed extension to passive phase conjugation (PPC) array equalisation [1], which we call PPC-DD. PPC equalises the difficult channels of shallow-water acoustic telemetry, readily exploiting diversity without the explicit data deconvolution many traditional equalisers would attempt. This equalising behaviour is argued from a deterministic, modal decomposition viewpoint in [1]. PPC match-filters the sensor signals and combines them into a single waveform. In PPC-DD this signal is quantised, giving a symbol estimate block that feeds back to a channel impulse response (CIR) estimator, producing filter coefficients needed in the next block. CIRs are tracked over the packet, in contrast with purely data-aided methods (e.g. [2]), reducing training cost and decoupling packet size from channel variability. Block least squares (LS) estimation by LSQR [3], a type of conjugate gradient (CG), enables compliant channel tracking. This gives deterministic finite-window LS estimation (LSE), an attractive option to standard RLS or decision-directed LMS-based methods ([4] p. 773) characterised, respectively, by exponential windowing and a statistical objective function. Adaptive filtering by CG was proposed earlier, e.g. [5]. Unlike many other array equalisers (e.g. [6]) no direct error signal feedback is used, and estimation is partitioned across channels. This avoids joint multi-channel optimisation, so complexity is linear in the number of sensors. Residual ISI [4] in the soft output can be further mitigated by traditional equalisers or sequence estimation.

Algorithm: We use symbol-rate processing, and integer sample times commensurate with normalised frequency. Data packet $\{I_k\}_0^{N_c-1}$ utilises BPSK [4] signalling so $I_k \in \{\pm 1\}$. We have N_c receive sensors and one transmitter. The baseband fixed channel model for q th sensor signal $y^q(t)$ is $h^q(t) * I_t + v_{eq}^q(t)$ where $v_{eq}^q(t)$ is i.i.d. zero-mean spatially uncorrelated noise, and where the N_c CIRs $\{h^q(t)\}_{q=0}^{N_c-1}$, which include the transmit pulse, are required to